

GeoSTAR – A geostationary microwave sounder for the future

B. H. Lambrigtsen, S. T. Brown, S. J. Dinardo, T. C. Gaier, P. P. Kangaslahti, A. B. Tanner
Jet Propulsion Laboratory – California Institute of Technology, 4800 Oak Grove Drive, Pasadena,
CA USA 91109-8099

ABSTRACT

The Geostationary Synthetic Thinned Aperture Radiometer (GeoSTAR) is a new Earth remote sensing instrument concept that has been under development at the Jet Propulsion Laboratory. First conceived in 1998 as a NASA New Millennium Program mission and subsequently developed in 2003-2006 as a proof-of-concept prototype under the NASA Instrument Incubator Program, it is intended to fill a serious gap in our Earth remote sensing capabilities – namely the lack of a microwave atmospheric sounder in geostationary orbit. The importance of such observations have been recognized by the National Academy of Sciences National Research Council, which recently released its report on a “Decadal Survey” of NASA Earth Science activities¹. One of the recommended missions for the next decade is a geostationary microwave sounder. GeoSTAR is well positioned to meet the requirements of such a mission, and because of the substantial investment NASA has already made in GeoSTAR technology development, this concept is fast approaching the necessary maturity for implementation in the next decade. NOAA is also keenly interested in GeoSTAR as a potential payload on its next series of geostationary weather satellites, the GOES-R series. GeoSTAR, with its ability to map out the three-dimensional structure of temperature, water vapor, clouds, precipitation and convective parameters on a continual basis, will significantly enhance our ability to observe hurricanes and other severe storms. In addition, with performance matching that of current and next generation of low-earth-orbiting microwave sounders, GeoSTAR will also provide observations important to the study of the hydrologic cycle, atmospheric processes and climate variability and trends. In particular, with GeoSTAR it will be possible to fully resolve the diurnal cycle. We discuss the GeoSTAR concept and basic design, the performance of the prototype, and a number of science applications that will be possible with GeoSTAR. The work reported on here was performed at the Jet Propulsion Laboratory, California Institute of Technology under a contract with the National Aeronautics and Space Administration.

Keywords: Atmospheric sounding, microwave, GOES, Geostationary, aperture synthesis, STAR

1. INTRODUCTION

The National Oceanic and Atmospheric Administration (NOAA) has for many years operated two weather satellite systems, the Polar-orbiting Operational Environmental Satellite system (POES), using low-earth orbiting (LEO) satellites, and the Geostationary Operational Environmental Satellite system (GOES), using geostationary earth orbiting (GEO) satellites. Similar systems are also operated by other nations. The POES satellites have been equipped with both infrared (IR) and microwave (MW) atmospheric sounders, which together make it possible to determine the vertical distribution of temperature and humidity in the troposphere even under cloudy conditions. Such satellite observations have had a significant impact on numerical weather forecasting accuracy, especially in regions where in situ observations are sparse, such as in the southern oceans. In contrast, the GOES satellites have only been equipped with IR sounders, since it has not been feasible to build the large aperture system required to achieve sufficient spatial resolution with a MW sounder in GEO. As a result, and since most clouds are almost completely opaque at infrared wavelengths, GOES soundings can only be obtained in cloud free areas and in the less important upper atmosphere, above the cloud tops (i.e. less important in a weather context). This has hindered the effective use of GOES data in numerical weather prediction. Full sounding capabilities with the GOES system are highly desirable because of the advantageous spatial and temporal coverage that is possible from GEO. While POES satellites provide coverage in relatively narrow swaths, and with a revisit time of 12-24 hours or more, GOES satellites can provide continuous hemispheric or regional coverage, making it possible to monitor highly dynamic phenomena such as hurricanes. Such observations are also important for studies of atmospheric processes and climate variability.

Efforts are under way to enable IR-based soundings in partially cloudy scenes also, with so-called cloud clearing techniques and using ancillary information other than the MW observations that are commonly used for that purpose –

and progress is being made in this area. However, that only marginally improves the scope and coverage of IR sounders and still leaves fully cloudy areas and severe storms in particular uncovered. That is where the need for a MW sounder is the greatest and will have the largest impact. Millimeter-wave radiometers are also extremely sensitive to scattering caused by ice in precipitating systems and can be used to estimate rain rates and convective intensity – a capability of great importance for the nowcasting and forecasting of the intensity of tropical cyclones and mesoscale convective systems. It is for reasons such as these that there has long been and continues to be – despite the recent development of hyperspectral IR sounders – a strong interest in and desire for a GEO MW sounder.

2. BACKGROUND

The Geostationary Synthetic Thinned Aperture Radiometer (GeoSTAR) concept was first developed at the Jet Propulsion Laboratory in 1998 under the name Geostationary Synthetic Aperture Microwave Sounder (GEO/SAMS) in response to a NASA Research Announcement² soliciting innovative measurement concepts suitable for geostationary applications and intended for demonstration on the NASA New Millennium EO-3 mission – described in³. Similar to a concept then being studied in Europe called the Microwave Imaging Radiometer by Aperture Synthesis (MIRAS)⁴, which is now being implemented by the European Space Agency as the Soil Moisture and Ocean Salinity (SMOS) mission⁵, GEO/SAMS (and its successor GeoSTAR) synthesizes a large aperture to measure the atmospheric parameters at microwave sounding frequencies (i.e. 50 and 183 GHz) with high spatial resolution from GEO without requiring the very large and massive dish antenna of a real-aperture system. The MIRAS instrument operates at a much longer wavelength (L-band, near 1.3 GHz) and is intended to measure surface parameters from a LEO orbit – and therefore may not appear to have any relevance to the atmospheric sounding problem, but it was realized by JPL investigators that the MIRAS concept can be scaled. The ratio between GEO and LEO orbit altitudes (about 40) is nearly identical to the ratio between the MIRAS measurement frequency and MW temperature sounding frequencies (also about 40), and it was thought that an analogous approach could therefore be used to obtain high spatial resolution from GEO at 50 GHz, just as MIRAS is used to obtain high spatial resolution from LEO at 1.3 GHz. This idea was the basis for the initial proposal to NASA.

GEO/SAMS was one of four concepts selected for Phase-A studies⁶ but was ultimately not selected for implementation. Instead, the Geosynchronous Imaging Fourier Transform Spectrometer (GIFTS), an IR sounder, was selected. The GIFTS project has encountered a number of problems, ranging from technical to budgetary. As a result, the New Millennium EO-3 mission has been cancelled, and the instrument development was halted after an engineering model had been completed. This experience points out the challenge of going from a concept to a space mission in a single step, as had been the goal of this New Millennium Earth mission. In contrast, the New Millennium Space missions are typically intended to carry out space demonstration of new technology components and subsystems, rather than complete systems, and have been very successful and generally on schedule.

The aperture synthesis concept was again proposed in response to a 2002 NASA Research Announcement⁷, this time focusing on pre-mission technology development being sponsored by the NASA Instrument Incubator Program (IIP), a technology development program under the Earth-Sun Systems Technology Office (ESTO). GeoSTAR was selected⁸, and an effort was initiated in 2003 at the Jet Propulsion Laboratory to develop the required technology and demonstrate the feasibility of the synthetic aperture approach with a small ground based proof-of-concept prototype. The objectives were to reduce technology risk for future space implementations as well as to develop and demonstrate the measurement concept, test performance, evaluate the calibration approach, and assess measurement accuracy.

The GeoSTAR prototype has now been completed, although tests and analysis continue. Results to date are excellent, and this development can now be characterized as proof of the 2D aperture synthesis concept – the first such proof, since it had until very recently not been feasible to prototype MIRAS prior to space implementation, and other efforts to demonstrate 2D aperture synthesis have not been unambiguously successful. This constitutes a major breakthrough in remote sensing capabilities and also validates the prototyping methodology. Further technology development is under way, both as risk reduction and to enhance the measurement capabilities of the GeoSTAR system, but the very successful development and testing of the prototype have brought the GeoSTAR concept to the level of maturity required for a space implementation.

3. PERFORMANCE REQUIREMENTS

In developing the GeoSTAR technology and prototype, a notional space system performing at the same level as the Advanced Microwave Sounding Unit (AMSU) system now operating on NASA and NOAA polar-orbiting LEO satellites was used for design and sizing purposes. This is a crucial aspect that makes it possible to assess the performance in a meaningful way and transfer results directly to a space version. The notional operational GeoSTAR will provide temperature soundings in the 50-60 GHz band with a horizontal spatial resolution of 50 km and water vapor soundings and rain mapping in the 183-GHz band with a spatial resolution of 25 km. Radiometric sensitivity will be better than 1 K in all channels. These are considered to be the minimum performance requirements, but the first space implementation could be built to exceed this minimum performance. Table 1 summarizes the spectroscopic measurement specifications of the POES AMSU for tropospheric sounding. GeoSTAR is intended to operate with those same spectral channels, to allow use of the same geophysical “retrieval” algorithms and to provide “science continuity” between the two systems, as well as to enable cross-calibration. The intention is further to focus on the portions of the atmosphere where clouds are prevalent and IR sounders are not performing well – i.e. in the troposphere, particularly in the lower and mid-troposphere. The two highest-frequency 50-GHz channels listed in Table 1 provide sensing in the upper troposphere and are therefore of secondary importance in this context. The temperature fields there also have less spatial and temporal variability than in the lower atmosphere, which will be exploited in the design and operation of a space version of GeoSTAR.

Table 1. AMSU/GeoSTAR spectroscopic requirements

Band	Func	Channels					
50 GHz	T(z)	50.3	52.8	53.6	54.4	54.9	55.5
183 GHz	q(z)	167	183 ±7	183 ±3	183 ±1		

4. THE GEOSTAR CONCEPT

As illustrated schematically in Fig. 1, GeoSTAR consists of a Y-array of microwave receivers, where three densely packed linear arrays are offset 120° from each other. Each receiver is operated in I/Q heterodyne mode (i.e. each receiver generates both a real and an imaginary IF signal). All of the antennas are pointed in the same direction. A digital subsystem computes cross-correlations between the IF signals of all receivers simultaneously, and complex cross-correlations are formed between all possible pairs of antennas in the array. In the small-scale example of Fig. 1 there are 24 antennas and 276 complex correlations ($=24*23/2$). Accounting for conjugate symmetry and redundant spacings, there are 384 unique so-called uv-samples in this case. Each correlator and antenna pair forms an interferometer, which measures a particular spatial harmonic of the brightness temperature image across the field of view (FOV). The spatial harmonic depends on the spacing between the antennas and the wavelength of the radiation being measured. The complex cross-correlation measured by an interferometer, called the visibility function, is essentially the 2-dimensional Fourier transform of the brightness temperature. By sampling it over a range of spacings and azimuth directions one can reconstruct, or “synthesize,” an image by discrete Fourier transform. In Fig. 1, the left panel shows the distribution of receivers in the instrument’s aperture plane, and the right panel shows the resulting sampling points in spatial Fourier space i.e. in terms of spatial harmonics.

The smallest spacing of the sample grid in Fig. 1 determines the unambiguous field of view, which for GeoSTAR must be larger than the earth disk diameter of 17.5° when viewed from GEO. This sets both the antenna spacing and diameter at about 3.5 wavelengths, or 2.1 cm at 50 GHz, for example. The longest baseline determines the smallest spatial scale that can be resolved, which for the array in Fig. 1 is about 0.9° (i.e. $17.5^\circ/\sqrt{384}$). To achieve a 50 km spatial resolution at 50 GHz, a baseline of about 4 meters is required. This corresponds to approximately 100 receiving elements per array arm, or a total of about 300 elements. This in

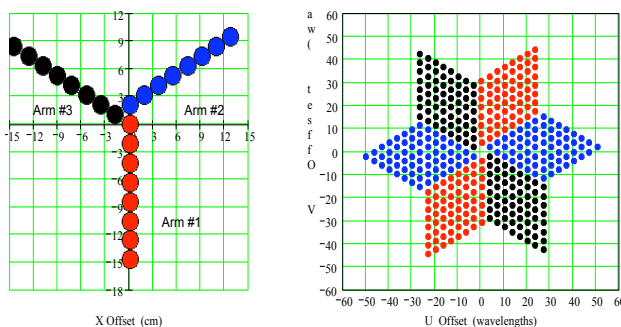


Fig. 1. Antenna array (left) and uv sampling pattern (right), as implemented in the GeoSTAR prototype

turn results in about 30,000 unique baselines, 60,000 uv sampling points (given conjugate symmetry), and therefore 60,000 independent pixels in the reconstructed brightness temperature image, each with an effective diameter of about 0.07° - about 45 km from GEO.

Fig. 2 shows the hexagonal imaging region (left panel) resulting from this star-shaped uv-sampling pattern imposed on the Fourier transform of the Earth brightness temperature field (right panel). As in all interferometric systems, there are “ghost” imaging hexagons adjacent to the primary one, and radiation originating from those areas is aliased into the primary area. However, in the GeoSTAR case this is not a problem since the space beyond the Earth disc is featureless and at a uniform 2.7 K temperature. (The sun and the moon will periodically be aliased into the imaging area, but those occurrences will be used to help calibrate the system.) As we discuss below, the primary imaging area can even be reduced somewhat to reduce the number of receiving elements needed to attain the required spatial resolution, and portions of the observations near the limb would then be contaminated by aliasing. That can be tolerated, however, since accurate sounding is limited to relatively high elevation angles. (Current LEO sounders and the algorithms developed for them typically cover elevation angles to about 30° ; it is likely that this can be extended to at least 20° .)

The system architecture is illustrated in Fig. 3. These illustrations represent the initial view of the aperture synthesis concept, as described in the original proposals. This view has evolved considerably during the prototyping effort.

In the small-scale example of Fig. 1 there are 10 antennas and 73 unique complex correlations, a number which accounts for redundant samples and conjugate symmetry. GeoSTAR is a spatial interferometric system that essentially operates in the spatial Fourier domain. Each correlator and antenna pair forms an interferometer, which measures a particular spatial harmonic of the brightness temperature image across the field of view (FOV). The spatial harmonic is determined by the spacing between the antennas and the wavelength of the radiation being measured. As a function of antenna spacing, the complex cross-correlation measured by an interferometer is called the visibility function (a term coined in the radio astronomy community, where related techniques have been used for many years). This 2-dimensional function is essentially the Fourier transform of the brightness temperature as a function of the incidence and azimuth angles. By sampling the visibility over a range of spacings and azimuth directions one can reconstruct, or “synthesize,” an image by discrete Fourier transform. In Fig. 1, the left panel shows the distribution of receivers in the instrument’s aperture plane, and the right panel shows the resulting sampling points in spatial Fourier space, i.e. in terms of spatial harmonics. Each cross in the sampling grid in Fig. 1 represents a location in Fourier space (traditionally called uv-space) and can be thought of as equivalent to a pair of terms in a sine/cosine expansion of the 2-dimensional radiometric field “function”. The cross-correlations are computed from both real and imaginary components of the received signal, and the visibilities (i.e. the “Fourier coefficients”) are therefore also complex and have two components at each uv sampling point. This corresponds to the cosine terms (real component) and the sine term (imaginary or quadrature component) of a Fourier series. Thus, the six uv points nearest the center of the diagram in Fig. 1 could be viewed as representing 2-dimensional a_1 and b_1 Fourier terms, and the next “ring” of uv points represent 2-dimensional a_2 and b_2 terms, etc. (Note that there is no sampling point at the center. That location corresponds to the a_0 term in a Fourier series, which represents the mean of the radiometric field. Its value is determined through separate means.)

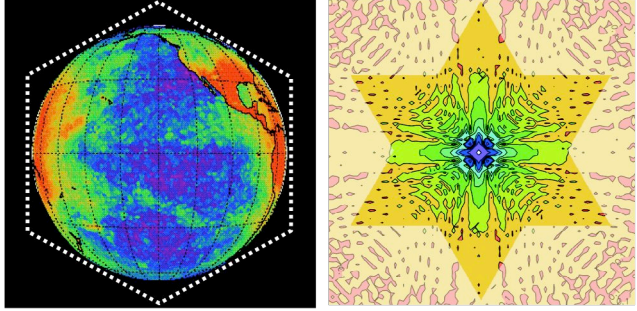


Fig. 2. Example brightness temperature image of Earth (left) and its Fourier transform (right). The uv sampling area from Fig. 1 is highlighted (right), and the resulting primary imaging region is outlined (left)

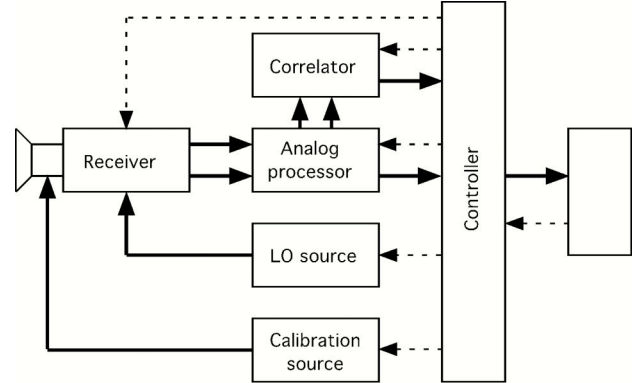


Fig. 3. Nominal system architecture

Each correlator and antenna pair forms an interferometer, which measures a particular spatial harmonic of the brightness temperature image across the field of view (FOV). The spatial harmonic is determined by the spacing between the antennas and the wavelength of the radiation being measured. As a function of antenna spacing, the complex cross-correlation measured by an interferometer is called the visibility function (a term coined in the radio astronomy community, where related techniques have been used for many years). This 2-dimensional function is essentially the Fourier transform of the brightness temperature as a function of the incidence and azimuth angles. By sampling the visibility over a range of spacings and azimuth directions one can reconstruct, or “synthesize,” an image by discrete Fourier transform. In Fig. 1, the left panel shows the distribution of receivers in the instrument’s aperture plane, and the right panel shows the resulting sampling points in spatial Fourier space, i.e. in terms of spatial harmonics. Each cross in the sampling grid in Fig. 1 represents a location in Fourier space (traditionally called uv-space) and can be thought of as equivalent to a pair of terms in a sine/cosine expansion of the 2-dimensional radiometric field “function”. The cross-correlations are computed from both real and imaginary components of the received signal, and the visibilities (i.e. the “Fourier coefficients”) are therefore also complex and have two components at each uv sampling point. This corresponds to the cosine terms (real component) and the sine term (imaginary or quadrature component) of a Fourier series. Thus, the six uv points nearest the center of the diagram in Fig. 1 could be viewed as representing 2-dimensional a_1 and b_1 Fourier terms, and the next “ring” of uv points represent 2-dimensional a_2 and b_2 terms, etc. (Note that there is no sampling point at the center. That location corresponds to the a_0 term in a Fourier series, which represents the mean of the radiometric field. Its value is determined through separate means.)

The smallest spacing of the sample grid in Fig. 1 determines the unambiguous field of view, which for GeoSTAR must be larger than the earth disk diameter of 17.5° when viewed from GEO[†]. This sets both the antenna spacing and diameter at about 3.5 wavelengths, or 2.1 cm at 50 GHz, for example. The longest baseline determines the smallest spatial scale that can be resolved, which for the array in Fig. 1 is about 2.0° (i.e. $17.5^\circ/\sqrt{73}$). To achieve a 50 km spatial resolution at 50 GHz, a baseline of about 4 meters is required. This corresponds to approximately 100 receiving elements per array arm, or a total of about 300 elements. That in turn results in about 30,000 unique baselines, 60,000 uv sampling points (given conjugate symmetry), and therefore 60,000 independent “pixels” in the reconstructed brightness temperature image, each with an effective diameter of about 0.07° - about 45 km from GEO.

5. PROTOTYPE DEVELOPMENT

The prototype was built to address the major technical challenges facing GeoSTAR and bring the maturity of the concept rapidly forward. These challenges are centered on the issues of system design and calibration. (Power consumption has also been a major concern, but because of continuing miniaturization of integrated circuit technology this is no longer viewed as a major issue.) Synthesis arrays are new and untested in atmospheric remote sensing applications, and the calibration poses many new problems, including those of stabilizing and/or characterizing the phase and amplitude response of the antenna patterns and of the receivers and correlators. To address these issues the prototype was built with the same receiver technology, antenna design, calibration circuitry, and signal processing schemes as are envisioned for the spaceborne system. Only the number of antenna elements is different. Thus, the prototype consists of a small array of 24 elements operating at 4 AMSU channels between 50.3 and 54.4 GHz. Fig. 4 shows a photo of it at an early stage of development.

The prototype design is based on aperture synthesis techniques originally developed for radio astronomy, and applied more recently to earth remote sensing. The first such application was the Electronically Scanned Thinned Array Radiometer (ESTAR)⁹, which was a 1-dimensional synthesis array operating at L-band to measure soil moisture. This small (5-element) aircraft system viewed a wide pushbroom swath, and was subject to a high degree of mutual coupling and array embedding effects that were difficult to model. This problem led to the so-called G-matrix calibration, where images are synthesized by inversion of interferometric fringes measured on an antenna range¹⁰. With this approach, the accuracy of the images depends on the quality of the antenna range measurements and the degree to which such measurements accurately represent the operational configuration (i.e. as installed in an aircraft or spacecraft structure). More recently, the European Space Agency’s MIRAS instrument, a 69-element system, is a 2-D imager configured as a Y-array of closely spaced patch antenna elements with a wide field of view (FOV) appropriate for low earth orbit. Like ESTAR, the broad antenna pattern of this system is subject to significant array embedding effects and mutual coupling which must be precisely measured and then accounted for in the inversion^{11, 12}. These measurements are quite costly and possibly even impractical. A large system with 300 elements or more is envisioned for each of two or three observation bands of GeoSTAR. It will be difficult to measure the G-matrix with very high precision for such a large array. Moreover, the inversion of such a large data set-- which would involve the inversion of a $30,000 \times 30,000$ matrix-- poses a major numerical-computational challenge.

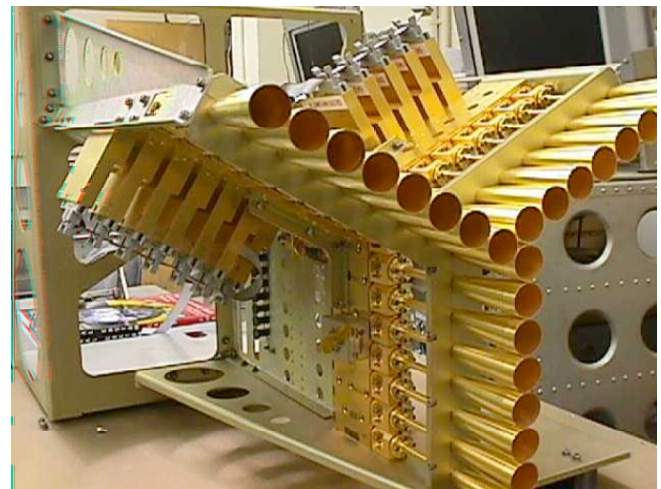


Fig. 4. GeoSTAR prototype – early stage

Our approach in GeoSTAR was to seek a design that does not depend so heavily on measurements of the antenna

[†] To be more precise: the unambiguous field must be larger than the area to be imaged for sounding purposes, which may be limited to the portion of the disc where the incidence angle does not exceed about 60° ; this is a diameter of about 14.5° , which would require an element spacing of about 4.5 wavelengths. For the prototype discussed here, 17.5° and 3.5 wavelengths were used, but a space version is likely to use the alternate numbers, which yield significant resource savings.

responses nor on the inversion of such large matrices. To the extent possible, we sought a design that could be characterized by a single well matched antenna pattern that is predictable and uniform among all elements of the array. If this could be achieved, the synthesis problem would become much simpler and could possibly be performed with a much more efficient Fast Fourier Transform rather than the computationally intensive G-matrix. One advantage with GeoSTAR is that observations of the Earth are made in a relatively small 17.5° wide FOV, the size of the Earth disc seen from GEO. (By comparison, the size of the Earth disc from LEO is about 130° .) This allows for a larger elemental antenna aperture, which offers more design options to reduce mutual coupling and other array embedding problems.

Perhaps the most important subsystem is the correlator, which must perform multiplications of all signal pairs in real time, each at a rate of about 100 MHz. For a spaceborne operational system with 100 elements per arm discussed earlier, that requires on the order of 20 trillion multiplications per second. To achieve such a high processing rate with a reasonable power consumption, the correlators are implemented as 1-bit digital multiply-and-add circuits using a design developed by the University of Michigan. 1-bit correlators are commonly used in radio astronomy. The correlator for the GeoSTAR prototype, where low cost was more important than low power consumption, is implemented in FPGAs. An operational system will use low-power application specific integrated circuits (ASICs). Current state of the art would then result in a power consumption of less than 20 W for the 300-element system discussed above, and per Moore's Law this will decline rapidly in future years.

During the buildup of the prototype, a number of component and subsystem tests were performed, which led to important design decisions. Both are key elements of a prototyping project, which have profound consequences for the viability and design of the eventual space instrument and also provide key information required for scaling, performance and tradeoff studies. These will not be discussed here – instead, we will concentrate on the various stages of system level testing.

6. FIRST LIGHT

The core of the prototype was completed in early 2005, and while some elements were still under development, system testing got under way as soon as that was feasible. The first real test of the system was performed by taking it outside, pointing it at a 45° angle at the sky and taking measurements as the sun transited through the field of view. At 50 GHz the sun has a brightness temperature of about 6000 K, which is reduced by atmospheric opacity to about 4000 K at 50.3 GHz. Since the sun is a very small source (about 0.5° diameter) viewed through wide-beam antennas (about 17° diameter beam width), the brightness temperature contrast against the sky measured by each receiver is only a few K. However, by measuring the cross-correlations it is possible to reconstruct radiometric images where the sun appears as a 4000 K bright spot. Fig. 5 shows the experiment setup (left panel) and one of the reconstructed images (right panel). The insert is a 3-dimensional representation of the radiometric response to this essentially point source. The “ghost images” are “sidelobes” that always appear in interferometry and are easily reduced to tolerable level by the application of so-called windowing functions or tapers.

The instrument was neither thermally shielded nor thermally controlled during this test (and the internal calibration system was not yet operational), and the sun caused significant heating. It was therefore very encouraging that the measurements demonstrated a very stable system that was able to operate well even under such harsh conditions. Nevertheless, a thermally controlled enclosure was constructed to allow subsequent precise performance assessments.

7. ANTENNA CHAMBER TESTS

The next set of tests were carried out at the NASA Goddard Space Flight Center, where a high quality compact antenna test chamber was made available for the purpose of determining the actual antenna patterns and allow comparisons with theoretical models. Fig. 6 shows the test setup (left panel) and a sample result (right panel). These results were also very encouraging and showed that the antenna patterns were of the required high quality, and the results closely matched the theoretical computations. A full analysis has also shown that the minor anomalies that are apparent in the antenna chamber measurements are largely due to minor antenna misalignments – a problem that is easily dealt with.

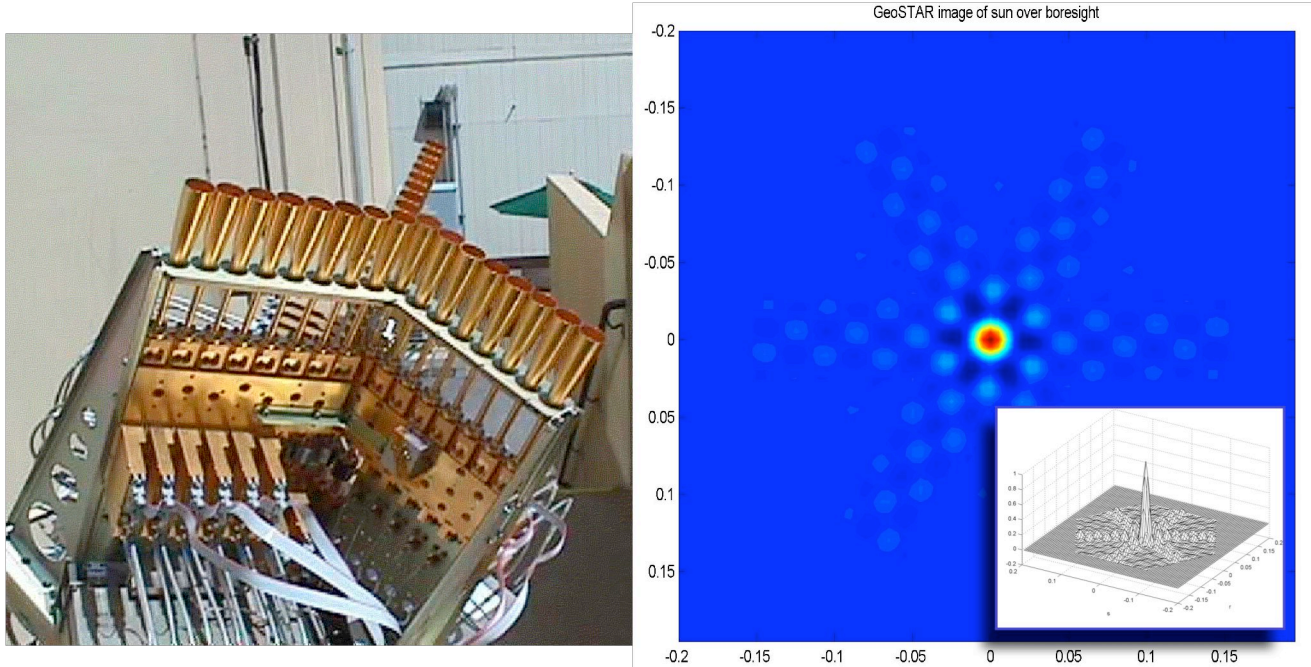


Fig. 5. Solar transit observations

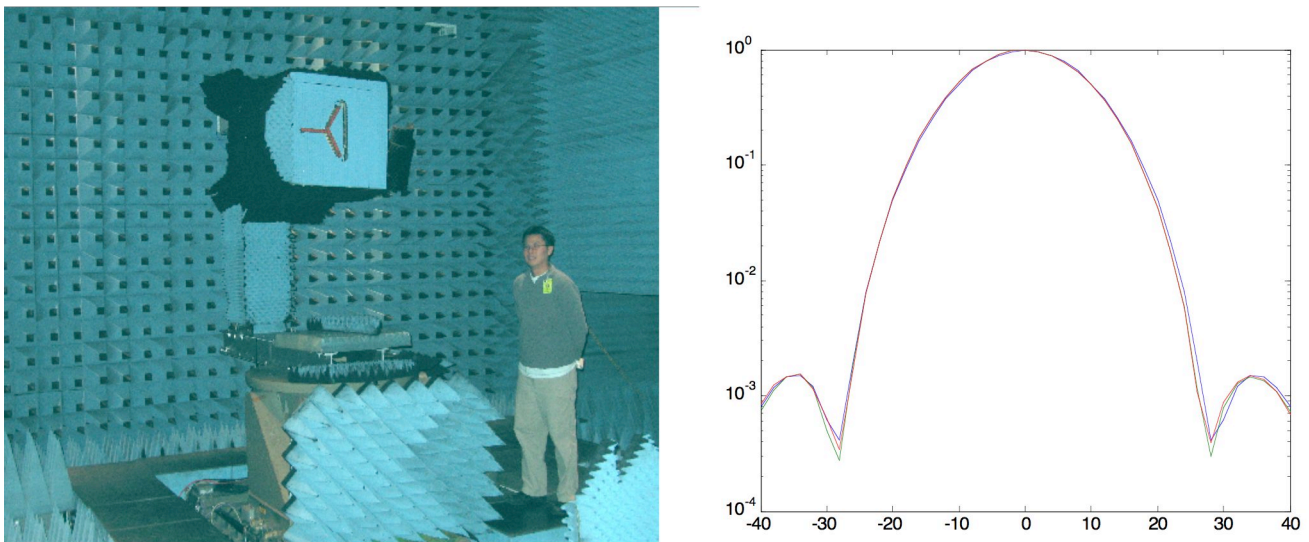


Fig. 6. Antenna chamber tests

Several months after the return of the prototype to JPL the antenna patterns were also measured by monitoring solar transits through the FOV. Analysis of those measurements showed identical results – including the same small anomalies that were revealed in the antenna chamber measurements. This shows that the system is stable over long periods (several months in this case) and is also mechanically robust (having traveled twice across the country and being packed and unpacked, moved around, etc.).

8. FIRST IMAGES

The next set of tests consisted of attempting to image natural radiometric scenes. For that purpose the prototype was again taken outdoors and pointed toward a series of hillsides at JPL. This yielded a remarkable set of images – the first successful imaging at 50 GHz with an aperture synthesis system. Fig. 7 shows an example – the left panel is a photo of the scene and the right panel is the reconstructed radiometric image at 50.3 GHz. The hexagonal outlines indicate the

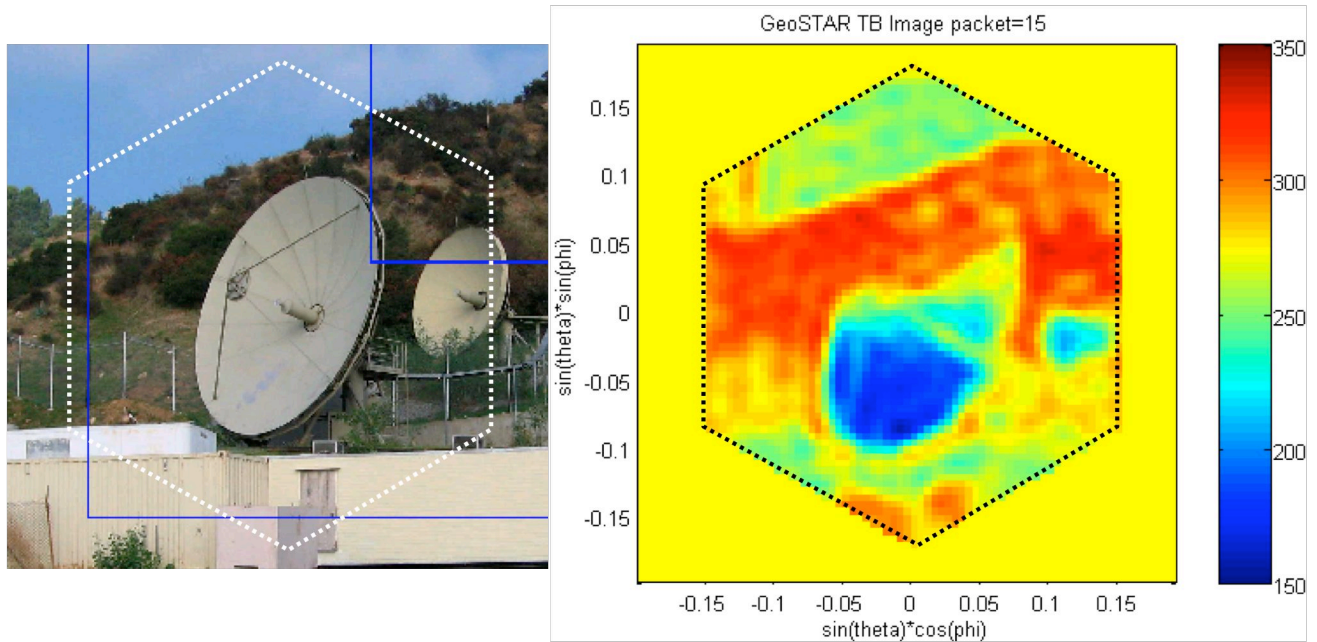


Fig. 7. First image of a natural source

primary imaging area. In an interferometric system such as GeoSTAR there are periodically replicated aliasing windows in the surrounding region. Radiometric sources within those windows will alias into the primary imaging area, and those effects are detectable in the images obtained in this series of tests. However, it should be noted that the prototype is sized for imaging from the geostationary vantage point, where there are no sources outside the primary imaging area – except for a uniform cosmic background (at 2.7 K) and occasionally the sun or the moon. The aliases created of both bodies will be used for calibration purposes and do not pose a problem.

These results represent a significant achievement with a relatively simple prototype system and demonstrate that the aperture synthesis approach works well on the type of radiometric source GeoSTAR is intended to observe.

9. NEAR FIELD IMAGING

The next step was to attempt quantitative measurements with a known and well characterized target. However, such a target would have to be in the far field of the instrument, which is several hundred feet. Arranging a controlled target large enough to subtend 17.5° and finding a large enough test range would be a major problem. To solve that problem, a transformation between near-field and far-field measurements was developed. This was first tested in a laboratory setting, and the results were very satisfactory. This worked so well that a “portrait studio” was rigged up. Fig. 8 shows an

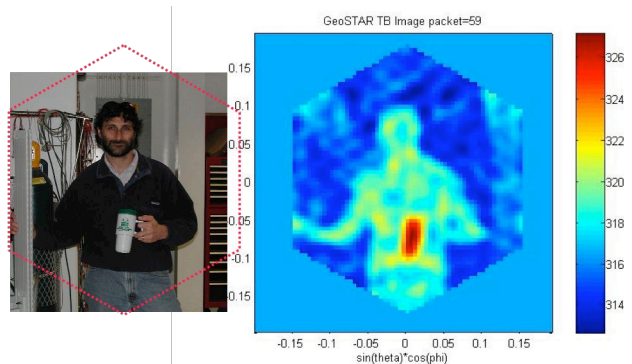


Fig. 8. Imaging in the near field

example, again with a photo of the target in the left panel and the transformed and reconstructed radiometric image in the right panel. It may be noted that the coffee cup the subject is holding is made of plastic, which is transparent at 50 GHz, and it is essentially the temperature of the coffee that is sensed. It is clearly above body temperature.

10. CALIBRATION

The purpose of developing near field imaging capabilities was to simplify the development of a setup that could be used for absolute radiometric measurements and the determination of radiometric sensitivity as well as calibration accuracy. That effort was outside the scope of the NASA funded IIP project, which was then coming to an end. Fortunately, the team was able to continue that effort under sponsorship of JPL’s internal R&D program. For this purpose, a calibration target emulating the Earth as seen from GEO was developed. The target consists of a large disk covered with material that is very absorptive in the microwave part of the spectrum and has an emissivity very close to 1. The circular disk is sized such that it subtends 17.5° from about 10 meters away. Embedded in the target are two rectangular temperature controlled sections. Each can be controlled independently. This results in three well-defined areas with separate temperatures: ambient for most of the target and the two controlled temperatures. In addition, there is a point source embedded in the center of the disk. This system allows for imaging tests involving sharp temperature gradients and allows for testing of temporal response and radiometric sensitivity as a function of integration time. All are important performance measures and permit testing of the theoretical models as well.

Fig. 9 shows this – the left panel is a photo of the setup, and the right panel shows a sample measurement results. The insert in the left panel shows radiometric images with the point source operating – the upper one as it appears uncorrected and the lower one as it appears with the near-field transformation applied (i.e. as it would appear in the far field). The right panel shows a reconstructed and alias-corrected image where the two temperature controlled areas are at equal temperature (but higher than the ambient temperature of the rest of the target). The lower portion of the right panel shows a typical time sequence of the various temperatures – dotted lines represent measurements with embedded thermistors and solid lines represent temperatures derived from the GeoSTAR observations.

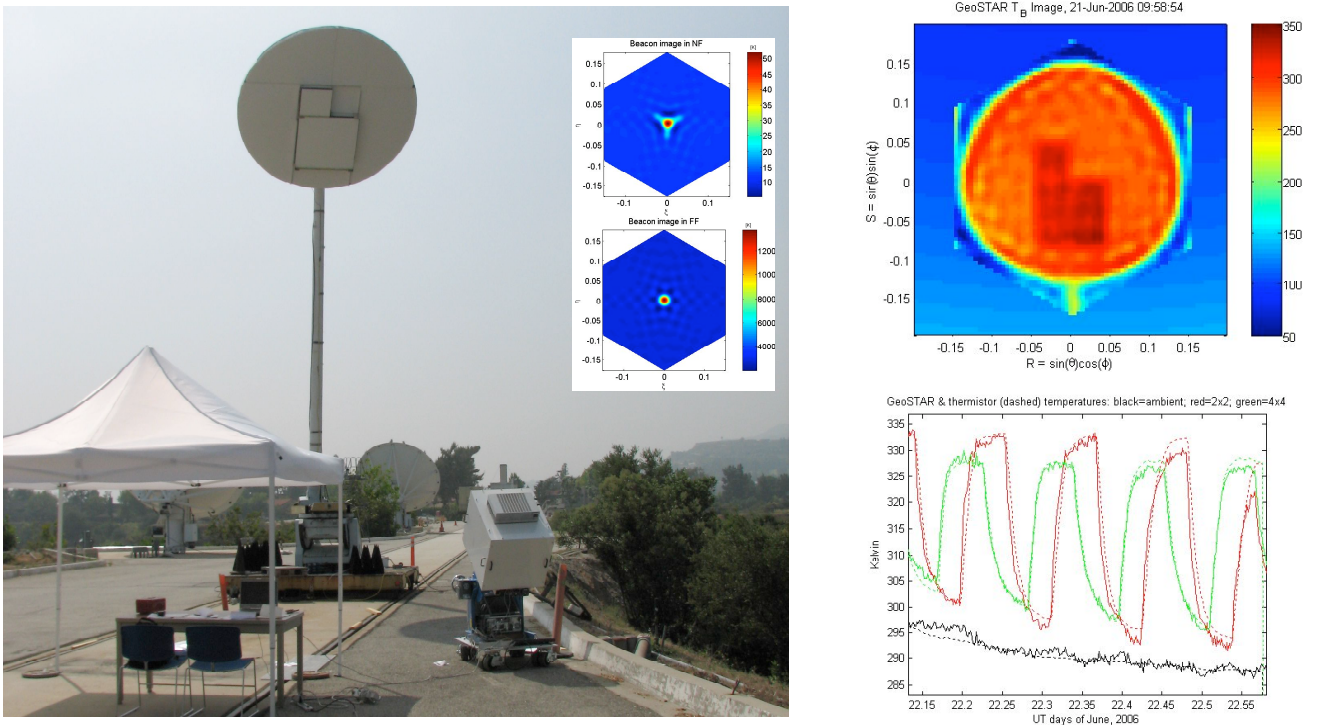


Fig. 9. Quantitative measurements on the JPL near-field range

11. SOUNDINGS AND SIMULATIONS

The next phase of quantitative assessment is just getting under way. Also sponsored under the JPL R&D program, it will consist of deploying the prototype in the field to make upward-looking temperature soundings of the lower atmosphere. The objective is to demonstrate sounding capability and to attempt to characterize the evolution of the temperature inversion that is frequently present in the Los Angeles area.

The final phase of the prototyping effort is also just getting under way. That will consist of the development of an end-to-end simulation capability, starting with realistic geophysical fields that would be observed from GEO and ending with retrieved geophysical fields and eventually a forecast assimilation system. When that final element is included, this is commonly called an Operational System Simulation Experiment (OSSE). These tools can be used to assess the impact of the observations without having to first invest in implementing a full space system. They can also be used to carry out performance and resource tradeoff studies. This is a crucial capability that complements a prototyping effort.

12. SUMMARY

The GeoSTAR concept and the related technology have been maturing rapidly – largely as a result of the prototyping approach¹³. The recent test results amount in effect to proof of concept, and this represents a major breakthrough in remote sensing capabilities. The prototype has also facilitated optimizing and further developing the dsystem design. The continuing efforts to develop the technology further, based on the tests and performance assessment of the prototype, will also enhance the system's performance as well as retire technology risk, and it is anticipated that the concept will be mature enough that a space mission can be implemented in the 2012-2015 time frame. The only major obstacles remaining will then be of a programmatic and budgetary nature. It is likely that those will be overcome, and so a GeoSTAR mission is likely within the next 10 years. This will add significantly to the nation's remote sensing capabilities, and the GeoSTAR observations are expected to have a significant forecast impact and will greatly benefit research related to the hydrologic cycle as well. In particular, the GeoSTAR observations will add much to our ability to observe, understand and predict severe storms, such as hurricanes.

The advantages of a synthetic aperture system over a real aperture system are significant. For example, error budget calculations based on simulations indicate that a synthetic aperture system can be expanded in size without unduly stressing the phase stability requirements. It is therefore well suited to meet future needs as the spatial resolution of numerical weather prediction models increase. Another advantage is that the GeoSTAR system does not require platform-disturbing mechanical scanning, and there is no time lag between different portions of the images, as there is in mechanically scanned real-aperture systems – where there can be a time lag of as much as an hour between the start of scan at the northern limit of the Earth disk and the end of scan at the southern limit. GeoSTAR thus produces true synoptic soundings; no other sounder has that capability. An additional advantage is fault tolerance. It is easy to add redundancy in the correlator system. Also, if one receiver should fail, the result is simply a slight degradation in image detail – there are no gaps in the image. (The reader can easily verify that by considering the effect of removing one receiver in Fig. 2.) This “graceful degradation” is in sharp contrast with the catastrophic failure modes of a conventional system, where the loss of one receiver will cause the loss of an entire sounding band.

REFERENCES

1. R. A. Anthes & B. Moore (eds.), *Earth Science and Applications from Space: National Imperatives for the Next Decade and Beyond*, National Research Council, National Academies Press, Washington, D.C., 2007
2. No author, “NRA-98-OES-12”, http://research.hq.nasa.gov/code_y/nra/current/NRA-98-OES-12/index.html (September 25, 1998)

3. B. H. Lambrigtsen, "GEO/SAMS – The Geostationary Synthetic Aperture Microwave Sounder", *Proc. IGARSS'00*, Vol. 7, 2984-2987 (2000)
4. M. Martín-Neira and J. M. Goutoule, "A two-dimensional aperture-synthesis radiometer for soil moisture and ocean salinity observations," *ESA Bull.*, no. 92, pp. 95–104 (1997)
5. P. Silvestrin, M. Berger, Y. Kerr and J. Font, "ESA's second Earth Explorer Opportunity mission: The Soil Moisture and Ocean Salinity mission—SMOS," *IEEE Geosci. Remote Sensing Newslett.*, no. 118, 11–14 (2001)
6. No author, "New Millennium Program in Support of the Office of Earth Science (OES) – NRA-98-OES-12", http://research.hq.nasa.gov/code_y/nra/current/NRA-98-OES-12/winners.html (March 3, 1999)
7. No author, "NRA-02-OES-02", http://research.hq.nasa.gov/code_y/nra/current/NRA-02-OES-03/index.html (July 16, 2002)
8. No author, "winners", http://research.hq.nasa.gov/code_y/nra/current/NRA-02-OES-03/winners.html (December 20, 2002)
9. C. S. Ruf, C. T. Swift, A. B. Tanner and D. M. Le Vine, "Interferometric synthetic aperture microwave radiometry for the remote sensing of the earth," *IEEE Trans. Geosci. Remote Sens.*, 26(5), 597-611, Sept. 1988.
10. A. B. Tanner and C. T. Swift, "Calibration of a Synthetic Aperture Radiometer," *IEEE Trans. Geoscience & Remote Sensing*, Vol.31, No. 1, Jan. 1993.
11. I. Corbella, F. Torres, A. Camps, A. Colliander, M. Martín-Neira, S. Ribó, K. Rautiainen, N. Duffo and M. Vall-llossera, "MIRAS End-to-End Calibration: Application to SMOS L1 Processor," *IEEE Trans. Geoscience & Remote Sensing*, Vol. 43, No. 5, May 2005.
12. A. Camps, I. Corbella, F. Torres, N. Duffo, M. Vall-llossera and M. Martín-Neira, "The Impact of Antenna Pattern Frequency Dependence in Aperture Synthesis Microwave Radiometers," *IEEE Trans. Geoscience & Remote Sensing*, Vol. 43, No. 10, Oct. 2005.
13. A. B. Tanner et al., "Initial results of the Geostationary Synthetic Thinned Array Radiometer (GeoSTAR) demonstrator instrument," *IEEE Trans. Geosci. Remote Sens.*, vol. 45, no. 7, pp. 1947-1957, Jul. 2007

ACKNOWLEDGMENTS

This work was carried out at the Jet Propulsion Laboratory, California Institute of Technology under a contract with the National Aeronautics and Space Administration. We acknowledge the invaluable contributions from our partners, Jeff Piepmeier of the NASA Goddard Space Flight Center, Chris Ruf, Boon Lim and colleagues of the University of Michigan, and Francisco Torres of the Polytechnic University of Catalonia, Spain.